Clin Neuroradiol (2019) 29:351–357
https://doi.org/10.1007/s00062-018-0709-x

ORIGINAL ARTICLE

Cranial MR-guided Focused Ultrasound for Essential Tremor

Technical Considerations and Image Guidance

J. Levi Chazen[1] · Travis Stradford[1] · Michael G. Kaplitt[2]

Received: 17 April 2018 / Accepted: 6 July 2018 / Published online: 25 July 2018

Abstract
Magnetic resonance guided focused ultrasound (MRgFUS) recently received FDA approval for treatment of medically refractory essential tremor and significant progress continues to be made in operational protocols. To that end, the goal of this technical article is to illustrate current optimization strategies for preprocedural, intraprocedural, and postprocedural imaging, with a particular focus on technically challenging intraprocedural MRI to assess satisfactory ablation.

Keywords Magnetic resonance guided focused ultrasound (MRgFUS) · Essential Tremor

Preprocedure

Computed Tomography

Prior to performing the procedure, a patient's skull density ratio (SDR) must be determined, as this parameter impacts maximum achievable temperature and thus treatment efficacy [1–3]. Per Insightec (Haifa, Israel) guidelines, an SDR of 0.4 is recommended as a threshold for treatment, below which ablative temperatures are difficult to achieve; however, the absolute SDR threshold varies by institution and operator experience. In practice, minimum SDR ranges from 0.35 to 0.45 are used. In the author's experience, ablative temperatures can be achieved despite low SDR values at or slightly below 0.4 if a high percentage of elements are available for the treatment (generally greater than 900). As discussed below, 1024 maximum elements are available with the treatment array and elements are blocked if they traverse air-filled paranasal sinus or intracranial calcifications. Therefore, a patient with a high SDR but extensive intracranial calcifications and prominent pneumatized frontal sinuses may provide a more challenging treatment candidate than a patient with low SDR but minimal calcifications and hypoplastic frontal sinuses.

A non-contrast CT of the head is performed from the vertex to skull base using a 512×512 matrix at 1 mm reconstruction thickness with a bone algorithm. The imaging protocol and reconstructions must be carefully followed as variations can result in an erroneous SDR calculation, even if a thinner reconstruction algorithm is utilized (for example, 0.625 mm slice thickness). The axial images are roughly aligned to the anterior commissure-posterior commissure (AC-PC) plane. The SDR is calculated using the Insightec treatment planning software; SDR calculations account for variations in the Hounsfield units across the thickness of the calvarium. The SDR is a measure of skull attenuation variability; a heterogeneous skull with large differences in attenuation between the inner table, diploic space, and outer table will result in a lower SDR than a patient with an overall hypodense marrow-rich or diffusely sclerotic calvarium [4]. Low SDR values have also been associated with postprocedural skull lesions, the clinical significance of which is unclear [5].

The use of CT imaging is equally important for evaluating intracranial calcifications and the position of the frontal sinuses, both of which have to be excluded as no-pass re-

✉ J. Levi Chazen
jlc2008@med.cornell.edu

Travis Stradford
trs7005@nyp.org

Michael G. Kaplitt
mik2002@med.cornell.edu

[1] Department of Radiology, Weill Cornell Medicine, New York-Presbyterian Hospital, 525 East 68th Street, New York, NY 10065, USA

[2] Department of Neurosurgery, Weill Cornell Medicine, New York-Presbyterian Hospital, 525 East 68th Street, New York, NY 10065, USA

gions prior to treatment. The phased-array cranial MRgFUS treatment unit has 1024 available elements. Elements are excluded by these no-pass regions, membrane folds, and the geometry of the frame. Greater than 800 elements are recommended for treatment; below a 700 element threshold ablative temperature may not be achievable. The CT imaging should be visually inspected for otherwise benign conditions, such as hyperostosis frontalis interna that may necessitate exclusion of a large number of elements and make treatment challenging.

Magnetic Resonance Imaging

At our institution, preprocedure MRI is acquired on a 3 T platform (HD750; GE Healthcare, Milwaukee, WI, USA) with a 32-channel head coil; imaging parameters are outlined in Table 1. We employ similar high-resolution anatomic sequences used for functional neurosurgery planning, such as deep brain stimulation, with multiplanar T1 and T2 imaging aligned to the AC-PC plane. Additionally, a whole brain diffusion tensor imaging sequence is acquired and fused with the anatomic imaging for preoperative planning and targeting of the thalamic ventral intermediate nucleus [3]. Fiber tracking is performed using Brainlab iPlanNet Cranial v3.0 (Munich, Germany). Tractography of the corticospinal tract (CST), medial lemniscus (ML), and dentatorubrothalamic (DRT) tracts has been described previously ([6, 7]; Fig. 1). Briefly, the DTI (diffusion tensor imaging) and anatomic MR images are imported into Brainlab and eddy current correction is performed on the DTI data set. The B0 image from the DTI acquisition and axial high-resolution T2 spin-echo image are then carefully fused in Brainlab, first using the autofusion function and then manually adjusted with attention to the AC-PC plane. This step is critical to subsequent procedural planning and target measurements as errors in the fusion step, even by 1–2 mm, can yield an incorrect target since the fiber tracking is performed on the DTI data but the AC-PC identification and measurements are performed on the anatomic T2 sequence (Fig. 2). Recent postprocessing software innovations that correct for MR image distortion are anticipated to benefit the procedure planning and image fusion [8].

Tractograms of the CST, ML, and DRT are then generated. A fractional anisotropy threshold is set to 0.3 with a minimum fiber length of 90 mm. The CST is generated by 3-dimensional seeds placed in the precentral gyrus and cerebral peduncle, the ML by seeds in the postcentral gyrus and ipsilateral dorsal pons and the DRT by seeds in the precentral gyrus and red nucleus. At the AC-PC level, the DRT can be visualized nestled anteromedially to the posteriorly located ML and laterally positioned CST (Fig. 1). On a coronal view, the CST courses medially toward the cerebral peduncle as it descends, an important relationship that the operator must keep in mind during ablation. When the spot shape dips below the AC-PC plane, the CST becomes vulnerable at a more medial location than it is in plane with AC-PC.

At our institution, essential tremor Vim target selection is performed independently by the treating neurosurgeon (MGK) and neuroradiologist (JLC) using indirect (atlas-based) and direct (DTI-based) targeting methods, respectively. Overall, there is an excellent agreement between the targeting methods with direct DTI-based coordinates trend-

Table 1 MR imaging protocol. All imaging is performed with zero slice spacing on a 3-Tesla GE 750 MR platform

Sequence	Matrix	TR (ms)	TE (ms)	TI (ms)	Flip angle	FOV (cm)	Slice Thickness (mm)	Nex	Frequency direction	Imaging options	Approximate time (min)
Preprocedure and postprocedure											
3D Sagittal T2 CUBE	256×256	3000	70	None	Var	25.6	1	1	S/I	NPW, EDR, Fast, ZIP512, ZIP2, FR, ARC	4:45
3D Sagittal T1 BRAVO	256×256	10	Min	450	12	25.6	1	1	S/I	EDR, Fast, IrP, ZIP2, ARC	4:25
Axial T2 FSE	384×256	3490	110	None	142	24	2	1	A/P	FC, EDR, TRF, Fast, FR	3:45
Axial SWAN	320×224	Min	24	None	10	20	2	1	A/P	FC, Fast, ZIP2, Asset	3:30
Axial DTI (55-Direction)	128×128	7500	Min	None	N/A	23	1.8	1	R/L	EPI, DIFF, Asset	5:00
Intraprocedure											
Axial T2 FIESTA	288×224	15	Min Full	None	55	22	2	3	R/L	NPW, EDR, Fast, ZIP512, ZIP2	4:00
Axial T2 FSE	256×256	2500	100	None	111	32	5	6	R/L	NPW, EDR, TRF, Fast, ZIP512, FR	3:00
Axial Diffusion	128×128	4000	Min	None	N/A	32	3	6	R/L	EDR, EPI, DIFF	1:00

ARC auto-calibrating reconstruction for cartesian sampling, *ASSET* array spatial sensitivity encoding technique, *DIFF* diffusion, *EDR* extended dynamic range, *EPI* echo planar imaging, *FR* fast recovery, *NPW* no phase wrap, *TRF* tailored radio frequency, *ZIP* zero interpolation processing

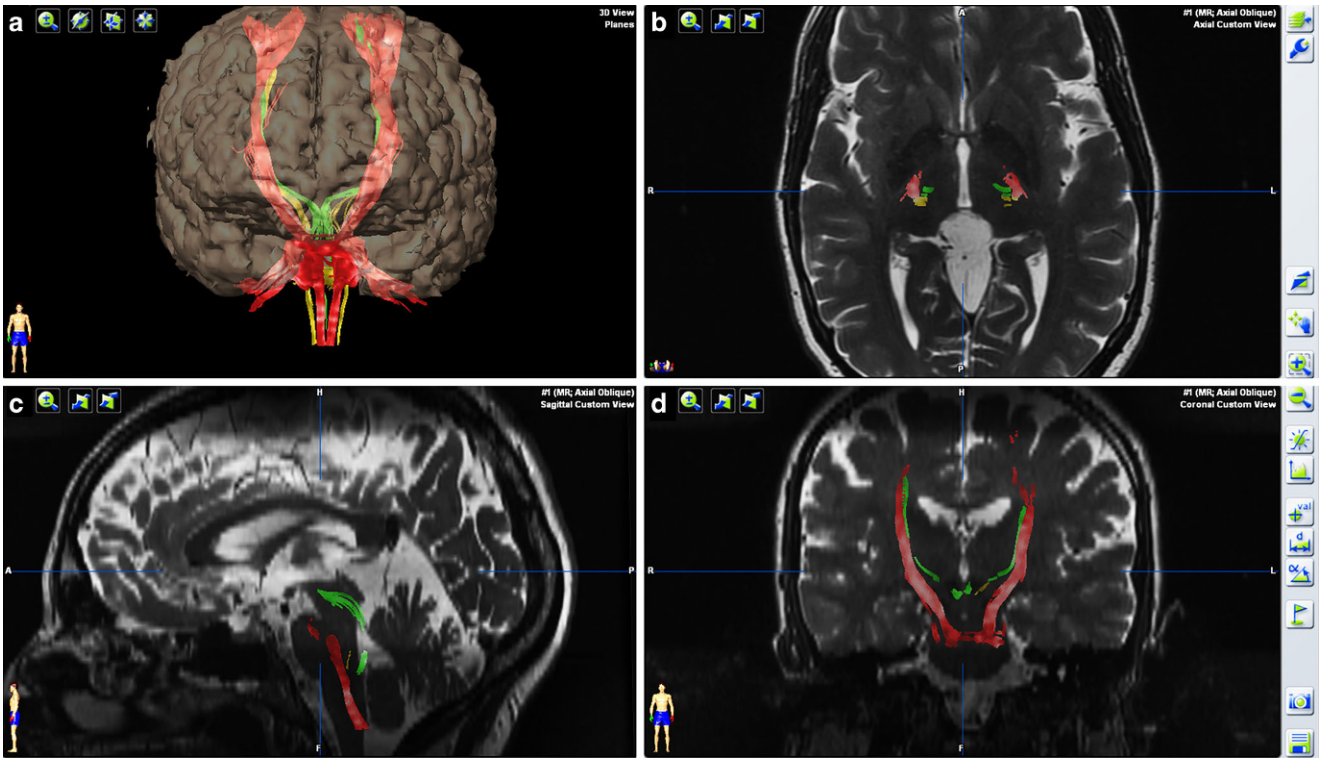

Fig. 1 3D (**a**), axial (**b**), sagittal (**c**), and coronal (**d**) reformations showing the corticospinal tract (*red*), dentatorubrothalamic tract (*green*), and medial lemniscus (*yellow*) for target planning. After careful co-registration of the anatomic T2 sequence with the DTI (diffusion tensor imaging) tractography, target selection can be performed

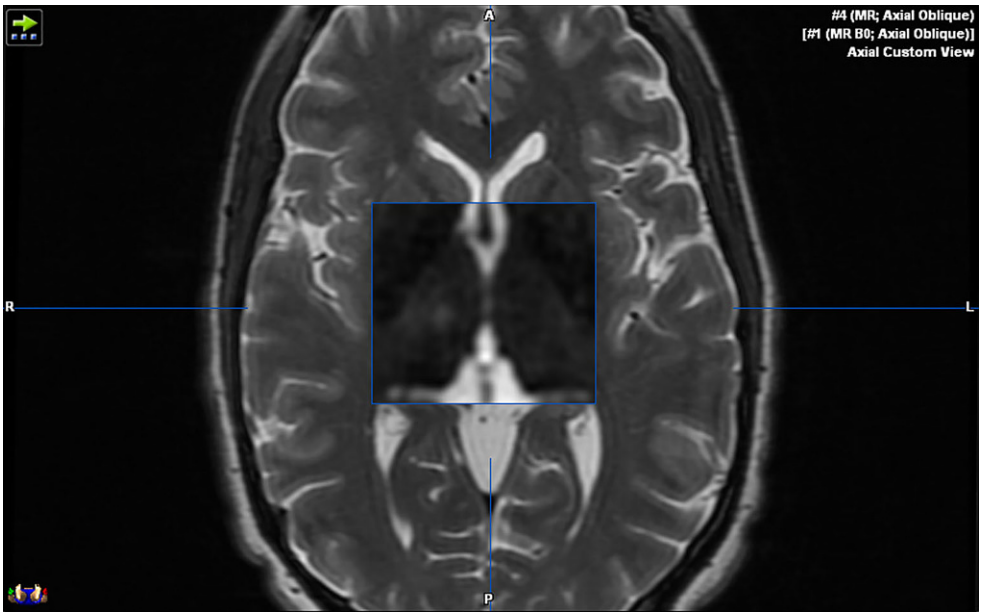

Fig. 2 Fusion image from Brainlab showing background T2 image with B0 overlaid (inside of *blue* box). By evaluating the ventricular margin and location of AC-PC, a careful fusion can be performed despite spatial warping inherent in the diffusion acquisition. This is a critical step for target planning and careful manual fusion should be performed

ing slightly medial and posterior to the indirect atlas-based target. In addition to aiding with initial target selection, DTI tractography provides invaluable information in relation to the borders of the ablation site. In the case of Vim thalamotomy, careful attention is required to avoid off target ablation of the CST laterally (that may result in a permanent motor deficit) and ML posteriorly (that may result in irreversible paresthesia). The size of the ablation spot can be inferred during the procedure using MR thermometry but the radius and margins of the ideal target are not readily apparent without the use of DTI tractography.

Intraprocedure

Intraprocedural imaging has the potential to aid both target localization and assessment of satisfactory ablation changes in the targeted thalamus; however, this imaging step presents unique challenges given the lack of a head coil on the Food and Drug Administration (FDA) approved 3 T system (ExAblate; Insightec, Haifa, Israel) and presence of a water bath surrounding the patient's scalp. Presently, intraprocedural cranial imaging must be performed with the body imaging coils embedded in the table as a head coil cannot be combined with the water bath and phased array treatment helmet [9]. When the patient arrives for treatment, the head is shaved and a four-point fixed cranial frame is applied with MRI-compatible plastic screws. An angulation is applied to the frame with elevation of the frontal screws relative to the occipital screws. The patient is then brought into the MRI suite and the frame is fixed into a water tight membrane that is filled with distilled, deoxygenated and cooled water. Following a baseline assessment of the patient tremor with an Archimedes spiral test and straight-line drawing, the procedure is commenced. A scout localizer is performed and three planes of anatomic T2 sequences are acquired for co-registration of the procedure imaging with the pre-procedure MRI and CT. The T2-weighted FIESTA sequences appear to provide the best image quality with the water bath/body coil system (Fig. 3). We enable the ZIP2 parameter on the MRI scanner for the FIESTA acquisition to generate 1 mm thin slices in three planes for procedure planning. Some operators suggest performing the initial procedural anatomic imaging before the water bath is filled for improved fidelity but we have not found this to be a helpful step. Once the T2 imaging is acquired, the target is prescribed in the AC-PC plane and co-registration is performed with the pre-procedure MRI-CT fusion. This fusion step may be time-consuming but care should be taken to manually align the imaging for the best possible fusion to ensure proper phase correction and optimal energy delivery. The treatment system then triggers triplanar motion detection MRI sequences and low-energy calibration sonications can then be initiated. We typically use an initial sonication energy of 250 W for a 10 s duration (2500 joules) to evaluate temperature response. The response is highly variable based on SDR, number of available elements, and cranial geometry but initial heating of approximately 45 °C is ideal to evaluate the spot shape. There are a number of nuances in the determination of spot shape; the plane of 2D MR thermometry must be varied during the treatment and frequency phase direction alternated to evaluate the 3D configuration of energy delivery [10]. A temporal mask can be applied if excessive medial-lateral smearing of the spot shape is present; the mask has the added advantage of decreased vertiginous symptoms during the sonication by reducing energy delivered through the inner ear.

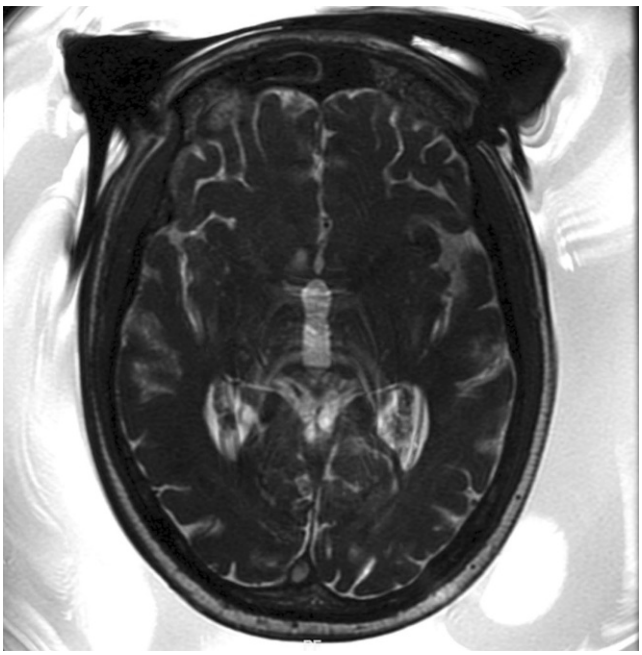

Fig. 3 T2-weighted FIESTA (Fast Imaging Employing Steady-state Acquisition) imaging with frame and water bath in place demonstrating optimal imaging of the AC-PC despite the absence of a dedicated head coil. Although there is significant wrap and ghosting artifact in the axial plane, the AC and PC are well delineated along with the margins of the third ventricle, permitting accurate targeting based on preoperative coordinates

Following successful sonication, the patient is re-evaluated for signs of paresthesia, language or motor disturbance and tremor response is assessed with serial spiral and straight line drawings. If no clinical response is elicited when >50 °C ablations are achieved on MR thermometry, target adjustment is likely required. Typically, we begin slightly (0.5–1 mm) anterior and medial to the ideal ablation target to allow a margin for irregular spot shape. After safe sonication at the desired temperature, the spot is usually adjusted slightly posterior with careful attention paid to clinical signs of paresthesia that could indicate encroachment upon the ML.

Intraprocedural MR imaging of the ablation is helpful at this juncture to confirm successful energy delivery and measure the ablation site relative to AC-PC. Up to this point in the treatment, the ablation site is determined relative to pre-ablation anatomic imaging and MR thermometry correlation. As such, the intraprocedural MR imaging provides the first true ablation response in real-time. Imaging in this setting with the water bath and lack of head coil presents a number of technical challenges that can be overcome with careful MRI technique. In addition to the decrease in signal to noise ratio (SNR) secondary to using a standard body coil, the dimensions of the water bath change the shape

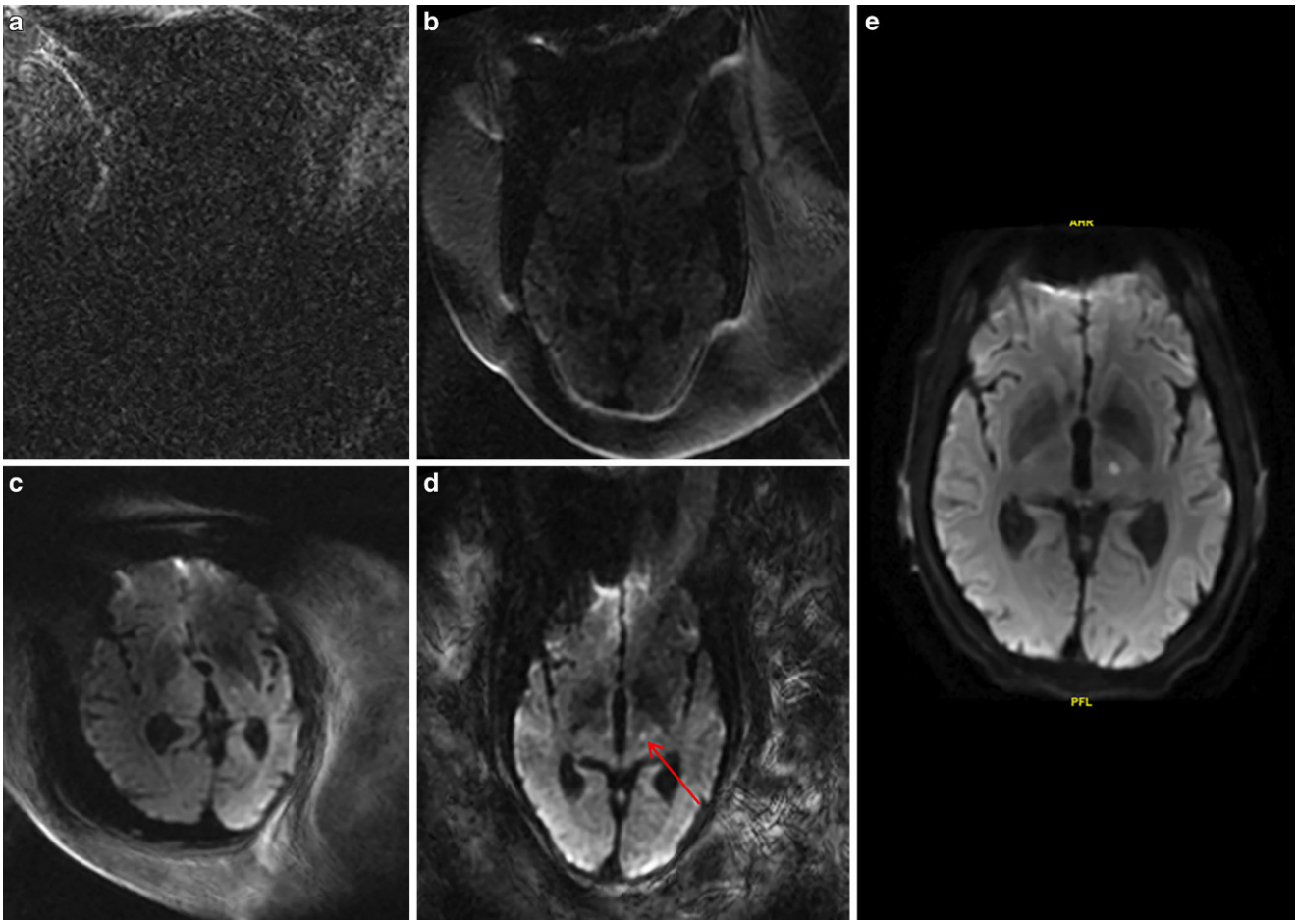

Fig. 4 Diffusion weighted imaging acquired during procedure (**a–d**) and immediately post-procedure (**b**). **a** Shows standard clinical diffusion sequences with a 22 cm FOV and 2 N_{EX} resulting in significant image distortion with water bath and non-head coil. **b** Image quality is improved by increasing FOV to 32 cm and N_{EX} to 6 but distortion is present from R/L phase encoding. **c** Shows the significant artifact introduced in the diffusion trace map if fixation pins are included in the imaging volume. **d** Shows an optimized intraprocedural diffusion imaging with 32 cm FOV, 6 N_{EX}, and A/*P* phase encoding. The ablation site in the left Vim is well seen (*arrow*). **e** Post-procedural diffusion imaging for comparison

of the target of interest from the normal oblong shape of a skull to that of a circle. Switching phase encoding direction from right-left to anterior-posterior helps to decrease the phase wrap artifact in this environment [11]. An increased field of view above 24 cm typically used for brain imaging to 32 cm seems to be optimal and significantly improves the SNR [11]. The number of excitations (N_{EX}) are also increased with a limited number of prescribed slices to boost image quality without significant time penalty ([12]; Fig. 4). Importantly, the fixation pins should be excluded from the slices acquired as part of the intraprocedural diffusion-weighted imaging (DWI) as the trace diffusion image will average the susceptibility artifact. Finally, special attention should be paid to the shimming process prior to image acquisition; it is best that this is done manually to focus the shim volume to the brain rather than the entire brain-water bath volume [13]. The above general principles are most helpful with respect to obtaining diagnostic diffusion sequences; the same concepts are applied when acquiring the intraprocedural T2-weighted sequence.

For T2-weighted intraprocedural imaging, a 10–15 slice axial stack is prescribed through the AC-PC plane and SNR is maximized by using a 5 mm slice thickness, N_{EX} of 6. This increases imaging time to approximately 3 min but provides diagnostic intraprocedural images (Fig. 5). Typically, this step is performed late in the treatment when increased power delivery and ablation times necessitate a patient cool down exceeding 180 s. It is important to note that this step provides the first anatomic evaluation of lesion size in real time. Other imaging sequences used for procedural monitoring and energy delivery including MR thermometry only provide an estimate of lesioning based on gradient echo thermometry maps and phase shift relative to normal brain. The authors also find the intraprocedural imaging step useful when considering timing to conclude the treatment. For example, if a positive clinical response has been achieved and the intraprocedural T2-weighted imaging demonstrates

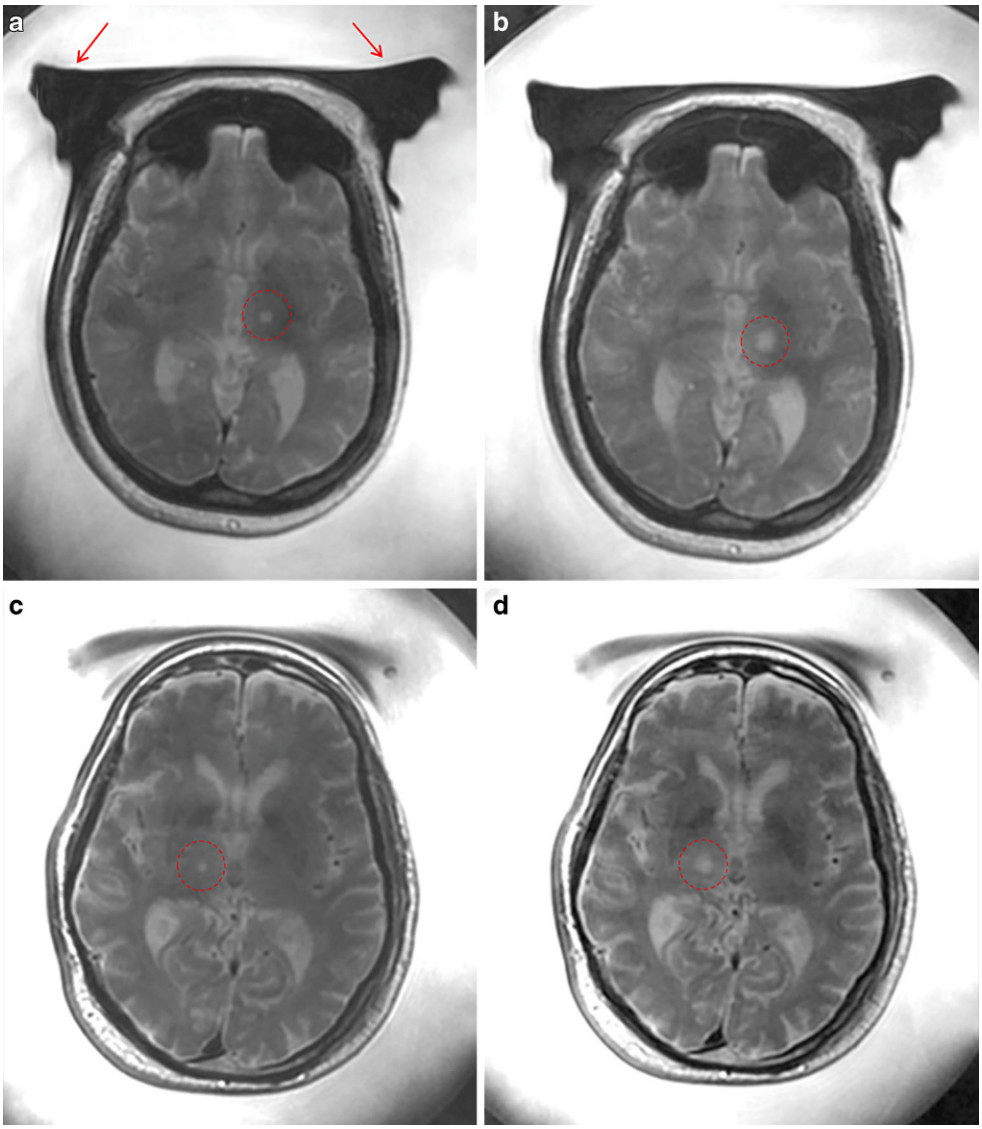

Fig. 5 Intraprocedural T2-weighted images acquired on two patients (**a**,**b** and **c**,**d**, respectively) with the head coil in place as evidenced by the T2 hyperintense extracranial water bath. The fixation pins are evident in the first patient (*arrows*, **a**). Images acquired mid-way through the procedure demonstrate a small T2 hyperintense ablation site (**a,c**) in the left and right Vim, respectively (*circles*). At the conclusion of the procedures, the T2 hyperintense ablation site had significantly expanded in both patients (*circles*, **b,d**)

a larger lesion with an edema halo greater than 5 mm, the procedure may be completed.

Postprocedure

Following the procedure, the water bath apparatus is drained, pins and frame removed, and a traditional head coil may now be used to acquire the postprocedural images. We typically acquire immediate postprocedural imaging for a posttreatment baseline. Perilesional edema will increase at 24 h and develop petechial microhemorrhage; the immediate postprocedure imaging demonstrates the most accurate lesion size before these changes occur [14]. We also perform a repeat DTI acquisition as part of the postoperative imaging, which shows targeted disruption of the DRT tremor circuit, potentially a useful outcome measure.

Patients are discharged home the same day and no procedural complications have been observed at our institution after treating over 25 patients with essential tremor to date.

Conflict of interest J. Levi Chazen, T. Stradford and M.G. Kaplitt declare that they have no competing interests.

References

1. Chang WS, Jung HH, Kweon EJ, Zadicario E, Rachmilevitch I, Chang JW. Unilateral magnetic resonance guided focused ultrasound thalamotomy for essential tremor: practices and clinicoradiological outcomes. J Neurol Neurosurg Psychiatr. 2014;86:257–64.
2. Elias WJ, Lipsman N, Ondo WG, Ghanouni P, Kim YG, Lee W, Schwartz M, Hynynen K, Lozano AM, Shah BB, Huss D, Dallapiazza RF, Gwinn R, Witt J, Ro S, Eisenberg HM, Fishman PS, Gandhi D, Halpern CH, Chuang R, Butts Pauly K, Tierney TS, Hayes MT, Cosgrove GR, Yamaguchi T, Abe K, Taira T, Chang JW. A randomized trial of focused ultrasound thalamotomy for essential tremor. N Engl J Med. 2016;375:730–9.

3. Chang WS, Jung HH, Zadicario E, Rachmilevitch I, Tlusty T, Vitek S, Chang JW. Factors associated with successful magnetic resonance-guided focused ultrasound treatment: efficiency of acoustic energy delivery through the skull. J Neurosurg. 2016;124:411–6.
4. Yamada K, Akazawa K, Yuen S, Goto M, Matsushima S, Takahata A, Nakagawa M, Mineura K, Nishimura T. MR imaging of ventral thalamic nuclei. AJNR Am J Neuroradiol. 2010;31:732–5.
5. Schwartz ML, Yeung R, Huang Y, Lipsman N, Krishna V, Jain JD, Chapman MG, Lozano AM, Hynynen K. Skull bone marrow injury caused by MR-guided focused ultrasound for cerebral functional procedures. J Neurosurg. 2018 May 4 [Epub ahead of print]
6. Chazen JL, Sarva H, Stieg PE, Min RJ, Ballon DJ, Pryor KO, Riegelhaupt PM, Kaplitt MG. Clinical improvement associated with targeted interruption of the cerebellothalamic tract following MR-guided focused ultrasound for essential tremor. J Neurosurg. 2017 Oct 20 [Epub ahead of print]
7. Sammartino F, Krishna V, King NK, Lozano AM, Schwartz ML, Huang Y, Hodaie M. Tractography-based ventral intermediate nucleus targeting: novel methodology and Intraoperative validation. Mov Disord. 2016;31:1217–25.
8. Calvo-Ortega JF, Mateos J, Alberich Á, Moragues S, Acebes JJ, José SS, Casals J. Evaluation of a novel software application for magnetic resonance distortion correction in cranial stereotactic radiosurgery. Med Dosim. 2018 May 8. [Epub ahead of print]
9. Elias WJ, Huss D, Voss T, Loomba J, Khaled M, Zadicario E, Frysinger RC, Sperling SA, Wylie S, Monteith SJ, Druzgal J, Shah BB, Harrison M, Wintermark M. A pilot study of focused ultrasound thalamotomy for essential tremor. N Engl J Med. 2013;369:640–8.
10. Rieke V, Instrella R, Rosenberg J, Grissom W, Werner B, Martin E, Pauly KB. Comparison of temperature processing methods for monitoring focused ultrasound ablation in the brain. J Magn Reson Imaging. 2013;38:1462–71.
11. Morelli JN, Runge VM, Ai F, Attenberger U, Vu L, Schmeets SH, Nitz WR, Kirsch JE. An image-based approach to understanding the physics of MR artifacts. Radiographics. 2011;31:849–66.
12. Mirowitz SA. MR imaging artifacts. Challenges and solutions. Magn Reson Imaging Clin N Am. 1999;7:717–32.
13. Rajiah P, Bolen MA. Cardiovascular MR imaging at 3 T: opportunities, challenges, and solutions. Radiographics. 2014;34:1612–35.
14. Wintermark M, Druzgal J, Huss DS, Khaled MA, Monteith S, Raghavan P, Huerta T, Schweickert LC, Burkholder B, Loomba JJ, Zadicario E, Qiao Y, Shah B, Snell J, Eames M, Frysinger R, Kassell N, Elias WJ. Imaging findings in MR imaging-guided focused ultrasound treatment for patients with essential tremor. AJNR Am J Neuroradiol. 2014;35:891–6.